

A learning agent that acquires social norms from public sanctions in decentralized multi-agent settings

Eugene Vinitsky^{1, 2}, Raphael Köster¹, John P. Agapiou¹, Edgar Duéñez-Guzmán¹, Alexander Sasha Vezhnevets¹ and Joel Z. Leibo¹

¹DeepMind, ²UC Berkeley

Society is characterized by the presence of a variety of social norms: collective patterns of sanctioning that can prevent miscoordination and free-riding. Inspired by this, we aim to construct learning dynamics where potentially beneficial social norms can emerge. Since social norms are underpinned by sanctioning, we introduce a training regime where agents can access all sanctioning events but learning is otherwise decentralized. This setting is technologically interesting because sanctioning events may be the only available public signal in decentralized multi-agent systems where reward or policy-sharing is infeasible or undesirable. To achieve collective action in this setting we construct an agent architecture containing a classifier module that categorizes observed behaviors as approved or disapproved, and a motivation to punish in accord with the group. We show that social norms emerge in multi-agent systems containing this agent and investigate the conditions under which this helps them achieve socially beneficial outcomes.

Keywords: Social norms, Multi-agent reinforcement learning, Social Dilemmas

1. Introduction

Autonomously operating learning agents are becoming more common and this trend is likely to continue accelerating for a variety of reasons. First, cheap sensors, actuators, and high-speed wireless internet have drastically lowered the barrier to deploy an autonomous system. Second, autonomy creates the possibility of learning “on device”, keeping experience local and off of any central servers. This makes it easier to comply with privacy requirements (Kairouz et al., 2019) and increases robustness by removing a single point of failure. Third, the autonomous approach is a potentially better fit for never-ending life-long learning (Platanios et al., 2019) since it does not require periodic syncing with updated centralized models. Indeed fully autonomous agents do not require any train-test separation at all, a property thought to be important for establishing open-ended autotrain (Leibo et al., 2019; Stanley, 2019).

However, the presence of multiple interacting autonomous systems raises a host of new challenges. Autonomously operating learning agents must be robust to the presence of other learning agents in their environment (e.g. Carroll et al. (2019); Crandall et al. (2018)). A significant issue that arises in the case of autonomous and decentralized learning agents is how to align their incentives. Achieving coordination is often hopeless when agents all may prefer selfishly to maximize their own rewards at one another’s expense. For instance, autonomous vehicles from multiple competing technology companies must share the road with one another and with human drivers (e.g. Liang et al. (2019)). Each car (company) “wants” to “selfishly” transport its users as quickly as possible. However, road congestion emerging from poor coordination negatively affects everyone. Human users also participate in these multi-agent systems, with even more autonomy. For instance, city neighborhoods compete with each other to reshape their roadways to incentivize driving apps to route traffic to

other neighborhoods (Çolak et al., 2016). Fundamentally, in collective action problems, letting agents egoistically optimize their own reward leads to a worse outcome for everyone than if all cooperate. This problem is particularly difficult if different ways to cooperate exist and agents have divergent preferences over the outcomes. In this case, *uncoordinated* cooperation may be no better than mutual defection. In these cases it is difficult for a consensus to emerge.

To tackle these social dilemmas we take inspiration from a mechanism that human societies use to resolve some of the collective action problems they face: *social norms*—group behavior patterns that are underpinned by decentralized social sanctioning (reward and punishment) (Balafoutas et al., 2014; Fehr and Fischbacher, 2004; Wiessner, 2005). Social norms enable cooperative behavior in a wide variety of collective action problems which otherwise would fail due to free-riding and defection. Human civilization is thick with social norms (Henrich and Muthukrishna, 2021; Tomasello and Vaish, 2013; Young, 2015). They are critical to our welfare because they discourage harmful behaviors (e.g. smoking in public places) and encourage beneficial behaviors (e.g. charitable donation and voting) (Bicchieri, 2016; Nyborg et al., 2016). Social norms are also important components in institutional solutions to small community scale natural resource management problems (Hadfield and Weingast, 2013; Ostrom, 2009) and aid large-scale collective actions like labor negotiations and democratic elections (Granovetter, 1978; Marwell and Oliver, 1993; Olson, 1965; Ostrom, 1998).

The critical assumption that will enable our agents to learn social norms by decentralized multi-agent reinforcement learning is that of *public sanctioning*. In this paradigm, there are discrete events when agent i makes their disapproval of agent j known by “punishing” them. These events are considered to be public so learning may be conditioned on knowledge of all sanctioning events from any agent to any other agent¹. This paradigm has several positive features. For instance, it allows for the possibility of human participants sanctioning autonomous machines through the same “API” that the machines use to sanction one another. For instance, human drivers and self-driving cars could honk at each other or leave 1-star reviews. As sanctions occur and are stored, databases of sanctioning events could enable agents to adapt to local customs like differing driving patterns between cities.

We construct an agent architecture that can use public sanctions to spark the emergence of social norms in a multi-agent reinforcement learning system. Our approach, which we call *Classifier Norm Model (CNM)*, mimics some of the key features that give efficacy to human social norms. First, social norms divide behavior into approved and disapproved categories. That is, they are classifiers (Hadfield and Weingast, 2014). Each agent has its own private representation of the group’s schema for what constitutes approved behavior. In our model, agents view other actors in the scene and generate a prediction for whether society at large would approve or disapprove of their behavior (Boyd and Mathew, 2021). Second, we assume that both human and artificial agents are intrinsically motivated to disapprove of behaviors that their group disapproves of (Boehm, 2012; Fehr and Fischbacher, 2004; Xiao and Houser, 2005).

We show that **CNM** magnifies emergent joint activity patterns that arise by chance in early exploratory learning. This “bandwagon” effect simultaneously pushes agents to cooperate and encourages them to cooperate in the same way as one another. Thus it mitigates the two fundamental dilemmas within each collective action problem: the start-up and free rider problems (terminology from Marwell and Oliver (1993)). In two complex collective action problems, we show that groups of **CNM** agents acquire beneficial social norms that decrease free-riding and coordinate cooperative actions, thereby causing higher per-agent returns. Next, we consider our results in light of arbitrariness properties of real-world social norms. That is, specific norms are not always beneficial relative to

¹This approach is related to, but not the same as, the longstanding AI recipe wherein a human operator could train a robotic learning agent through the use of a “deliver reward now” button, making AI training similar to animal training (Walter, 1951). Our setting differs since we make all sanctioning events *publicly* available to all learners.

counterfactual situations where other norms prevail (different ways of cooperating) [Bicchieri \(2016\)](#); [Ostrom \(2009\)](#). This is a key property of real-world norms and our model also captures it. Finally, we analyze the CNM agent architecture with ablation experiments to understand which architectural assumptions are key to our results.

2. Related work

Significant progress in multi-agent reinforcement learning has occurred over the last few years driven by rapid innovation in a paradigm where researchers assume that even though policies must ultimately be executed in a decentralized manner (without communication at run time), they can be trained offline beforehand in a centralized fashion. This paradigm is called centralized training with decentralized execution (CTDE) ([Baker, 2020](#); [Foerster et al., 2018b](#); [Iqbal and Sha, 2019](#); [Lowe et al., 2017](#); [Rashid et al., 2018](#); [Sunehag et al., 2018](#)). Many algorithms in this class take an actor-critic approach and employ a centralized critic that takes in observations from all agents to produce a single joint value ([Baker, 2020](#); [Lowe et al., 2017](#)). One algorithm called OPRE maintains the division between training and test phases but does not learn a centralized critic. Instead in OPRE each agent learns its own critic but all critics are conditioned on the observations of the other players. This is interpreted as information available in “hindsight” ([Vezhnevets et al., 2020](#)). Other techniques make extensive use of the centralized regime by expanding and pruning the support of policies in each rollout; this includes algorithms like PSRO ([Lanctot et al., 2017](#)) and XDO ([McAleer et al., 2021](#)).

A rather different class of models takes the approach of constraining the *kind* of information that can be communicated between agents, instead of constraining the time (training time versus test time) of its communication. These models avoid the need for explicit training and testing phases. They can be executed online and maintain full decentralization except for the specific data they need to communicate. Some researchers have studied the case where no information at all is communicated between agents. However this approach cannot usually resolve social dilemmas or coordinate on beneficial equilibria when multiple equilibria exist unless special environmental circumstances prevail ([Köster et al., 2020b](#); [Leibo et al., 2017](#); [Pérolat et al., 2017](#)). A few algorithms eschew training/testing but still cannot be considered fully decentralized since they require each player to be able to access the policies of other players ([Foerster et al., 2018a](#); [Jaques et al., 2019](#)). Most algorithms in this class that can robustly find socially beneficial equilibria in collective action problems require public rewards ([Eccles et al., 2019](#); [Gemp et al., 2020](#); [Hughes et al., 2018](#); [McKee et al., 2020](#); [Peysakhovich and Lerer, 2018](#); [Wang et al., 2019](#)) or the ability to redistribute rewards amongst agents’ ([Lupu and Precup, 2020](#); [Wang et al., 2021](#)). This class of algorithms assumes that while they are learning all agents will have real-time access to one another’s rewards².

However, making reward data public is undesirable for several reasons. (A) Agent designers may want to alter reward functions without affecting the larger multi-agent system. (B) Agent designers may be prohibited from sharing their agents’ reward function on privacy grounds, for instance, if they constructed it from individual user data ([Kairouz et al., 2019](#)), or their reward functions may be proprietary. (C) Humans may inhabit the same multi-agent system as artificial agents. This is most apparent in autonomous vehicle applications. Humans cannot publicize their instantaneous reward signals, but both human-driven and self-driven cars can honk their horn to admonish others for bad driving.

In the real world, social norms need not be beneficial. For example they may ossify inefficient economic systems or unfairly discriminate against classes of people ([Akerlof, 1976](#); [Bicchieri, 2016](#);

²or near real-time, some algorithms use temporally blurred reward signals from the other players ([Hughes et al., 2018](#); [McKee et al., 2020](#); [Wang et al., 2019](#)).

Mackie, 1996). In other cases, social norms can be “silly rules” that are neither directly harmful nor helpful (Hadfield-Menell et al., 2019; Köster et al., 2020a). Yet some social norms are clearly helpful, like those that discourage harmful behavior. There are two main mechanisms through which beneficial social norms function: (A) stabilizing cooperation in social dilemma situations as the sanctioning can transform the payoffs into a game with new equilibria (Kelley et al., 2003; Ullmann-Margalit, 1977/2015) and (B) equilibrium selection. Here the question is how it can be predicted which equilibrium a society will select, given that multiple equilibria exist for the social situation in question (e.g. Lewis (1969)). In this case the norm is a piece of public knowledge on which individuals may condition their behavior to rationally coordinate their actions with one another (Gintis, 2010; Hadfield and Weingast, 2012; Vanderschraaf, 1995). Naturally, these two functions are often intertwined (e.g. (Bicchieri, 2006)). In this spirit, social norms have been treated in AI research as equilibria of repeated normal form games (Sen and Airiau, 2007; Shoham and Tennenholtz, 1997).

Recent work has aimed to study social norms in more complex models of human societies. One line of research has represented social norms with classifiers that label a behavior’s social approval or disapproval. For instance, Boyd and Mathew (2021) studied how such a classifier can interact positively with a reputation-based account of cooperation in iterated matrix games and Köster et al. (2020a) demonstrated the potential benefits of a “hand-crafted” (i.e. not learned) classifier on the learning dynamics of enforcement and compliance behavior in multi-agent reinforcement learning.

3. Multi-agent reinforcement learning with sanctions

3.1. Definitions

The formal setting for multi-agent reinforcement learning with sanctions is an N -player partially observed general-sum Markov game (e.g. Littman (1994); Shapley (1953)) augmented with a shared sanctioning observation.

At each state $s \in \mathcal{S}$ of a Markov game, each player $i \in I = \{1, \dots, N\}$ takes an action $a_i \in \mathcal{A}_i$. Players cannot perceive each state directly, but instead receive their own d -dimensional partial observation of the state $o_i \in \mathbb{R}^d$, which is determined by the observation function $\mathcal{O} : \mathcal{S} \times I \rightarrow \mathbb{R}^d$. After the players’ joint action $\vec{a} = (a_1, \dots, a_N)$, the state changes according to the stochastic transition function $\mathcal{T} : \mathcal{S} \times \mathcal{A}_1 \times \dots \times \mathcal{A}_N \rightarrow \Delta(\mathcal{S})$, where $\Delta(\mathcal{S})$ denotes the set of discrete probability distributions over \mathcal{S} . After each transition, each player i receives a reward $r_i \in \mathbb{R}$ according to the reward function $\mathcal{R} : \mathcal{S} \times \mathcal{A}_1 \times \dots \times \mathcal{A}_N \times \mathcal{S} \times I \rightarrow \mathbb{R}$.

We extend this standard definition to include an additional *sanctioning observation* that is shared by all players. At each state, in addition to their individual observation o_i , each player i also receives a sanctioning observation $g \in \mathcal{G}$, defined by the sanction-observation function $\mathcal{B} : \mathcal{S} \rightarrow \mathcal{G}$. This observation broadcasts global information on sanctioning to all players.

3.2. Sanction-observation function

We define a *sanctioning opportunity* as a situation where one agent can observably sanction another agent by taking an action that causes them a reward or punishment³. These are often situations where agents are physically near one another, but in general they need not be. If an agent has a sanctioning opportunity and chooses to punish the other agent with its next action, we call this a *disapproval event*. If the agent has a sanctioning opportunity but does not choose to punish the other

³Aficionados will already know this, but it’s worth pointing out for anyone new to this terminology, the word ‘sanction’ is an auto-antonym. It means both approval and disapproval.

agent with its next action, we call this an *approval event*⁴. We use these events as the basis of our sanctioning observations.

Formally, for any given state $s \in \mathcal{S}$, let the set of sanctioning opportunities be given by $\mathcal{J}(s) \subseteq I^2$, where $(i, j) \in \mathcal{J}(s)$ whenever agent i has a sanctioning opportunity towards agent j . Note that $\mathcal{J}(s)$ may be empty if no agent has a sanction opportunity, and at the other extreme $\mathcal{J}(s) = I^2$ when every agent can sanction every other agent (including themselves). In this work, agents disapprove by emitting a zapping beam; a sanction opportunity (i, j) therefore exists only if agent i is physically in range to zap agent j .

Let $C(s, i, j)$ be the *context* of sanctioning opportunity $(i, j) \in \mathcal{J}(s)$ —the perspective of the decision-making agent leading up to its choice to approve/disapprove. In general, $C(s_t, i, j) = (o_{0:t}^{(i)}, a_{0:t-1}^{(i)})$, the full history of the decision-making agent’s individual observations and actions; however, it is also possible to use less context. For instance, in the environments we study here, agents change color as a function of their recent behavior. Thus it is sufficient to choose $C(s_t, i, j) = o_t^{(i)}$, the current observation of the agent with the sanctioning opportunity. E.g. think about a child stealing a cookie. If when you encounter them they still have chocolate all over their face then you need not have directly observed their transgression to disapprove of their behavior.

Finally, let $\mathcal{Z}(s, \vec{a}, i, j) \in \{0, 1\}$ be a binary indicator of whether the actions \vec{a} taken in state s resulted in a *disapproval* event (of j by i). In this work we define $\mathcal{Z}(s, \vec{a}, i, j) = 1$ if agent i zaps agent j .

Putting everything together, we get a sanction-observation function that, at time t , returns a global view of the sanctioning opportunities at time $t - 1$, the sanctioning decisions made at those opportunities, and the context for those decisions:

$$\begin{aligned} \mathcal{B}(s_{t-1}, \vec{a}_{t-1}) &= \{(i, j, c, z) \mid (i, j) \in \mathcal{J}(s_{t-1}) \wedge c \\ &= C(s_{t-1}, i, j) \wedge z = \mathcal{Z}(s_{t-1}, \vec{a}_{t-1}, i, j)\} \end{aligned}$$

This depends on the previous state s_{t-1} and actions taken \vec{a}_{t-1} , but can be represented as $\mathcal{B}(s_t)$ as desired by augmenting the state to include prior observations.

3.3. Learning social norms

In this work, we learn the social norm by training a classifier on the public sanctioning observations provided by $\mathcal{B}(s_{0:T})$. Given a classifier Ψ_ϕ that outputs probabilities of sanctioning and assuming the set of sanctioning opportunities is of size M , we form a binary cross-entropy loss

$$\mathcal{L}_\phi = \frac{1}{M} \sum_{c, z \in \mathcal{B}} -z \log(\Psi_\phi(c)) - (1 - z) \log(1 - \Psi_\phi(c))$$

and minimize this loss using stochastic gradient descent.

There are some potential challenges with learning this classifier. A key issue is that since the classification will be learned from data sampled from an episode, it is not clear what happens to the classifier predictions on unobserved events. For example, if a particular agent behavior is effectively

⁴Symmetrically, it is possible to define approval events to be when the agent with the opportunity takes an action to reward the other agent and disapproval events to be when it does not do so (positive sanctioning). However we do not consider that case here. We made this choice because the bulk of the literature on sanctioning and social norms is primarily concerned with negative sanctioning (cf. Baldwin (1971); Bicchieri et al. (2018)). Positive and negative sanctions are not equivalent to one another for a variety of reasons. One is that, from the perspective of society, negative sanctions are often cheaper to implement than positive sanctions since the latter requires coupling to some additional source of rewards that agents can “gift” to one another.

suppressed, the classifier will no longer receive samples of group approval / disapproval of that behavior and may experience *catastrophic forgetting* (McClelland et al., 1995) and unlearn its prior pattern of disapproval. For this reason, we stop classifier learning by setting the learning rate of the classifier to zero after some fixed number of time-steps. This freezes the group norm as observed by the classifier at that point in time but does not prevent subsequent drift in agent behavior.

3.4. Learning policies

The core idea of the **CNM** agent is that an individual embedded in a wider group is motivated to sanction in accord with the group’s joint pattern of approval and disapproval. This shapes the group’s behavior because disapproval is punishing.

The motivation to sanction in accord with the group’s norm is created by a pseudoreward term (i.e., an intrinsic motivation in the sense of Singh et al. (2004)):

$$\Omega_\phi(o_t, a_t) = \begin{cases} +\alpha & \text{if } a_t \text{ is disapproval} \wedge \Psi_\phi(o_t) \geq 0.5 \\ -\beta & \text{if } a_t \text{ is disapproval} \wedge \Psi_\phi(o_t) < 0.5 \\ 0 & \text{otherwise} \end{cases}$$

for $\alpha, \beta \in \mathbb{R}_0^+$. The *Classifier Norm Model* **CNM** agent learns the classifier and applies this pseudoreward in decentralized multi-agent reinforcement learning. Each agent i learns a parameterized behavior policy that is conditioned solely on the history of its own individual observations and actions and its estimate of the social norm $\pi_\theta(a_t^{(i)} | o_{0:t}^{(i)}, a_{0:t-1}^{(i)}, p_t)$ where $p_t = \text{stop}(\mathbb{1}[\Psi_\phi(o_t) \geq 0.5])$ and $\text{stop}(\cdot)$ is the stop gradient operator.

Both classifier and policy consist of a convolutional backbone attached to a multi-layer perceptron (MLP). The classifier MLP directly outputs the predictions whereas the policy MLP feeds into an LSTM whose outputs are the action probabilities. The classifier network takes the prior frame to make its prediction (context length is one, see Sec. 3.2) whereas the policy takes the current frame to get an action. Our classifier and policy do not share any layers in our basic architecture. The architecture, the manner in which predictions are passed to the policy, and the pseudoreward are depicted in Fig. 1.

Each agent’s policy is implemented using a private neural network, with no parameter sharing between agents. Each agent’s policy parameters are independently trained to maximize the policy’s long-term γ -discounted payoff:

$$V_{\theta, \phi}^{\vec{\pi}}(s_0) = \mathbb{E} \left[\sum_{t=0}^{\infty} \gamma^t \mathcal{R}_i(s_t, \vec{a}_t, s_{t+1}) + \gamma^t \Omega_\phi(o_{t-1}^{(i)}, a_{t-1}^{(i)}) \middle| \vec{a}_t \sim \vec{\pi}_t, s_{t+1} \sim \mathcal{T}(s_t, \vec{a}_t) \right],$$

where the pseudoreward term shapes sanctioning behavior towards coherence with the group’s pattern of approval and disapproval. To closely approximate this expectation, we train on episodes sampled from $\vec{\pi}$: all agents control exactly one player in every episode.

The reinforcement-learning algorithm used for each agent is A3C (Mnih et al., 2016) with a V-Trace loss for computing the advantage (Espeholt et al., 2018). To the standard A3C loss we add a contrastive predictive coding loss (Oord et al., 2018) in the manner of an auxiliary objective (Jaderberg et al., 2017a), which promotes discrimination between nearby timepoints via LSTM state representations. For more details, refer to the Appendix.

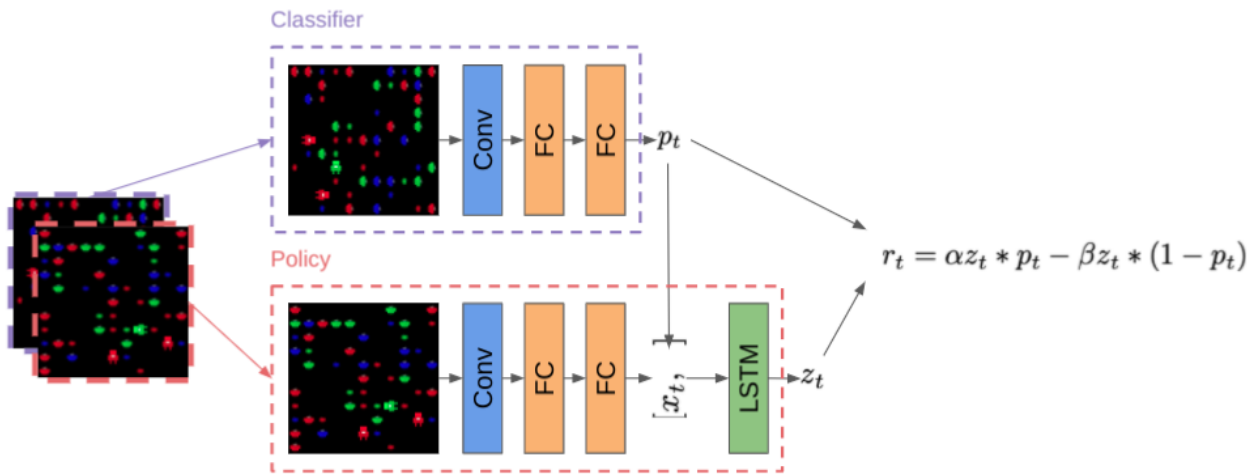


Figure 1 | Visual depiction of how the classification is done and how the pseudoreward for aligning with the classifier is generated. The frame at which disapproval occurs and the frame before are stacked together; the frame before the disapproval is fed into the classifier to generate a prediction. If the agent chooses to disapprove, then a reward or penalty is generated based on whether its choice aligns with its classifier prediction.

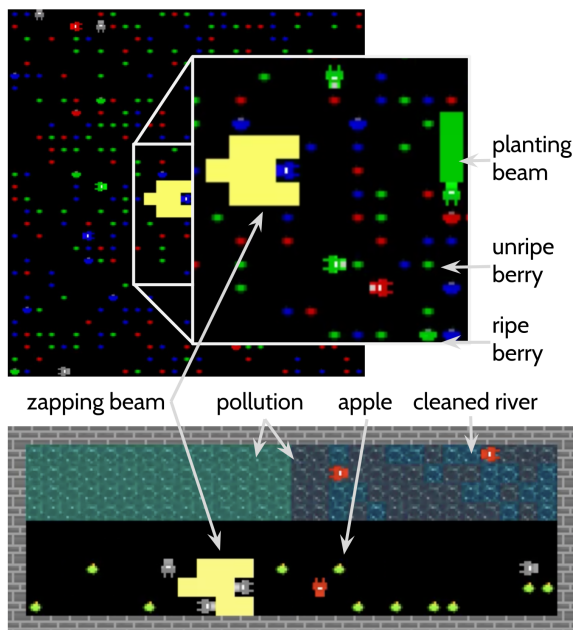


Figure 2 | **(Top)** Allelopathic Harvest. Agents can recolor (replant) berries using one of three colored beams; a green beam is shown here. An agent's color is given by the berry color they most recently changed a berry to be (planted) or stochastically reverts to gray upon eating a berry. They also can zap agents to punish them (yellow beam). **(Bottom)** Clean Up with Startup Problem. Agents have a cleaning beam that can be used to clean pollution on either side of the divide as well as having a zapping beam that they can use to punish agents.

4. Environments

We study two collective action situations (games) implemented in Melting Pot [Leibo et al. \(2021\)](#). The games are depicted in Fig. 2, *Allelopathic Harvest*⁵ (AH) and *Clean Up with Startup Problem* (CSP). Both contain several different equilibria, each associated with a distinct type of “work” and superior to other uncoordinated equilibria. Thus both games contain start-up and free-rider sub-problems (terminology from [Marwell and Oliver \(1993\)](#)). This means that in order to achieve high rewards the agents must distribute some amount of work among themselves (cooperate) and most of that work should advance the same unified goal (coordinate). Learning in both games may be decomposed loosely into two phases. First, before much learning has occurred, very few individuals work consistently toward any goal so defection is motivated by fear that too few others will contribute to successfully establish any norm (the start-up problem). In the later phase of learning, when most individuals are engaged, then the motivation to defect is greed since one can free-ride on the efforts of others ([Heckathorn, 1996](#)). Games with this collective action problem structure were previously studied with MARL in [Köster et al. \(2020b\)](#).

In *Allelopathic Harvest* (adapted from [Köster et al. \(2020b\)](#)), agents are presented with an environment that contains three different varieties of berry (red, green, and blue) and a fixed number of berry patches, which can be replanted to grow any color variety of berry. The growth rate of each berry variety depends linearly on the fraction that that color comprises of the total. As depicted in Fig. 2, agents have three planting actions with which they can replant berries in front of themselves in their chosen color. Agents in AH have heterogeneous tastes. Specifically, half the agents receive twice as much reward from eating red berries relative to other berries and the other half have preferences of the same form except that they favor green. Agents can achieve higher return by selecting just one single color of berry to plant, but which one to pick is difficult to coordinate (start-up problem). They also always prefer to eat berries over spending time planting (free-rider problem).

In *Clean Up with Startup Problem* (adapted from [Hughes et al. \(2018\)](#)), the agents need to coordinate on a specific type of pollution to clean out of two pollution types as is shown in Fig. 2. The environment contains apples that the agents are rewarded for eating, but the apple spawn rate increases monotonically with the ratio between the two pollution types. If the agents clean both pollution types equally, then apples will not spawn at all. Agents thus need to coordinate on a particular pollution type to clean (start-up problem) while also incentivizing enough agents to do the work of cleaning (free-rider problem).

Both environments have a rule with an effect similar to the cookie example from Sec. 3.2. Individuals can see which kind of work (or free riding) other individuals have recently been engaged in. They change color to reflect this information. This makes it easier for agents to identify free-riders and those planting prohibited berry varieties (AH) or cleaning the wrong kind of pollution (CSP). In both environments the agents are colored according to their most recent planting or cleaning action. For example, successful planting of a red berry (AH) or successful cleaning of red pollution (CSP) causes the agent itself to become red. Similarly, agents that eat fruit are colored grey to indicate that they have not recently planted or cleaned. Thus grey colored agents are typically free riding.

In both environments agents can zap one another at short-range with a beam. This serves as the punishment mechanism. Importantly, in both games there are also instrumental reasons for agents to zap one another, especially to compete for berries/apples. Getting zapped once freezes the zapped agent for 25 steps and applies a mark that indicates that the agent did something that was disapproved of (similar to [Köster et al. \(2020a\)](#)). If a second zap is received while the agent is

⁵see <https://youtu.be/1a24sFmk618> and <https://youtu.be/A4zMh9359r8> for videos of example episodes of AH and CSP, respectively. **Note for reviewers: these links are anonymized.**

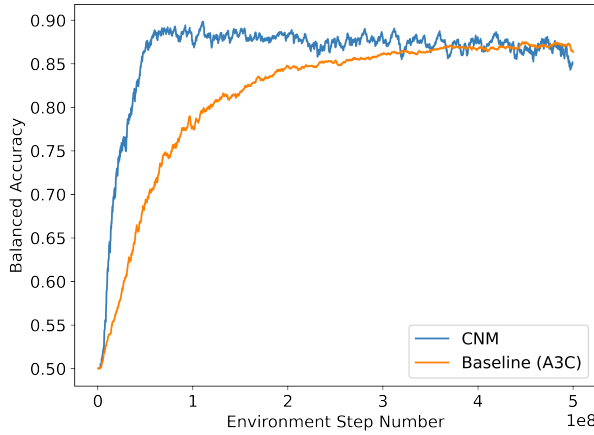


Figure 3 | The classifier achieves high balanced accuracy in predicting approval versus disapproval events (the average accuracy over both positive and negative samples).

marked, the agent is removed for 25 steps and receives a penalty of -10 . If no zap is received for 50 steps, the mark fades. For full details on the environment please refer to Appendix Sec. B.

5. Experiments

5.1. Existence and Beneficial Effects of the Emergent Social Norms:

In order to align themselves with the social norm, agents must first learn to represent it accurately. Fig. 3 shows the balanced accuracy of the classifier in two cases where pseudorewards are on and one where the classifier is left on but has no influence in the environment. We observe three features. First, we are able to rapidly learn a classifier that achieves high balanced accuracy. The fact that it is possible to achieve high accuracy despite using only a single frame suggests that the initial normative behavior is something simple like “zap an agent if it might compete with you over a visible berry” or “zap agents of a particular color”. Second, we note that the intrinsic motivation to punish in accord with the classifier’s predictions causes its accuracy to rapidly converge. This is because disapproval is punishing so agents adjust their behavior to be in accord with the classifier and thereby evade punishment. Finally, we freeze the classifier after $5e7$ steps, but despite this, the balanced accuracy remains relatively high for the duration of training, suggesting that there is not too much drift in the normative aspects of agent behavior after the freeze. Similar results were obtained for *CSP* as well.

Next, we investigate whether the use of **CNM** leads to better outcomes. In *AH* we run 20 seeds and in *CSP* we run 10 seeds. In *AH*, the measure of success is the *monoculture fraction*, the percentage of the color that corresponds to the largest number of berry spawning sites. Fig. 4b demonstrates that **CNM** increases the monoculture fraction above 50%, indicating that agents on average are converging to a single preferred color, and also increases the net agent return, indicating that the costs of norm enforcement (punishing violators) are overcome by increased berry consumption. Similarly, we observe that in *CSP* they are able to successfully select one of the two pollution types over the other. The inverted minimal fraction measures how imbalanced the two types of pollution are; higher inverted minimal fraction is desirable. The result is a significant consequent increase in collective return. Note that collective return includes the costs of being punished since these are externally imposed by other agents but does not include the pseudoreward term since it models an internal drive.

Groups of **CNM** agents display a bandwagon effect, magnifying weak patterns of sanctioning in

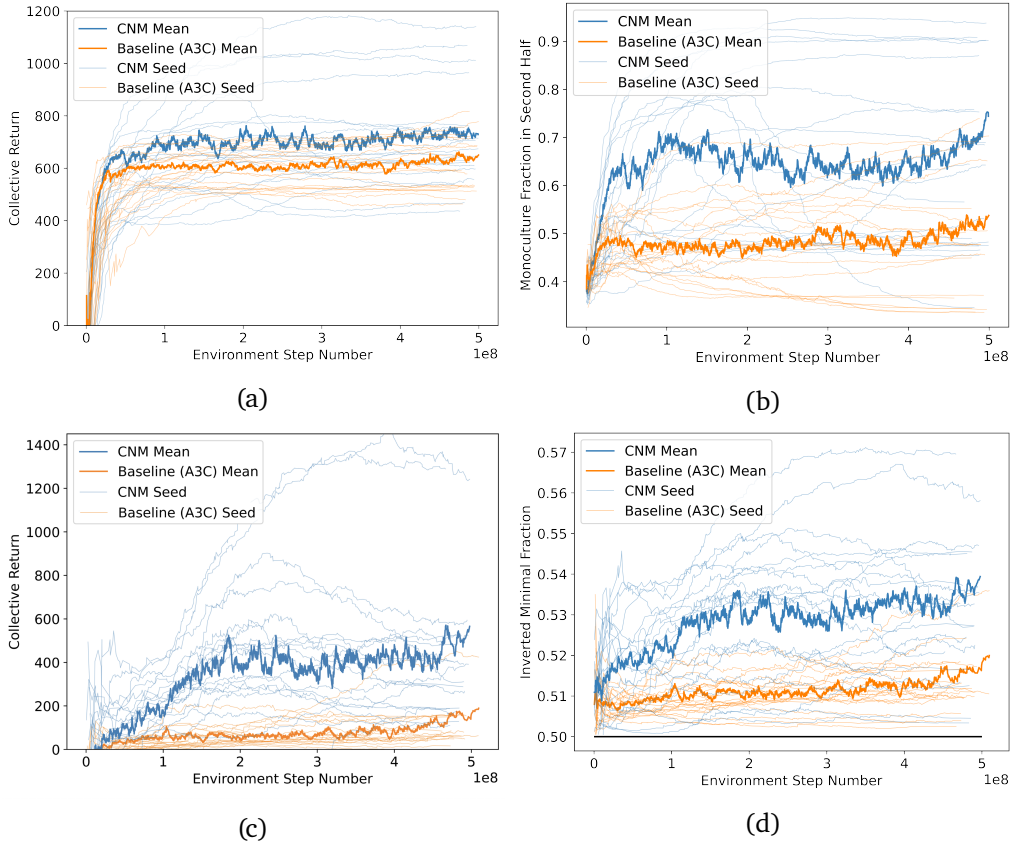


Figure 4 | The effect of norms on avoiding startup problems and overcoming freerider problems. The thick lines represent the mean across seeds while thin, transparent lines represent individual seeds; the standard deviation is not displayed for visual clarity. (a) Collective return in *AH*. (b) Fraction of total berries constituted by the dominant berry in the second half of the episode. (c) Collective return in *CSP*. (d) Average fraction of total pollution constituted by the dominant pollution type.

initially random exploratory behavior. They are more likely than the baseline to coordinate on a coherent joint behavior (planting a specific berry color in *AH* or cleaning a specific pollution type in *CSP*). But there is no guarantee that they will select the most beneficial equilibria available to them. This mirrors the arbitrariness of real-world social norms. For example, recall that all agents in *AH* prefer either red or green berries over blue berries (see Sec. 4). If agents have an early tendency to plant the undesirable blue berries and punish free-riders, then the classifier will learn to approve of these behaviors and the agents will stabilize on a blue equilibrium, an outcome that none of the agents prefer over the red or green equilibria. This is why there is so much variation in the outcomes achieved between independent runs (Fig. 4). See also Fig. 6 where the prevalence of blue berry centric outcomes can clearly be seen.

Finally, we confirm that the improvement in reward is not somehow occurring due to a suppression of the penalty action and a consequent decrease in penalty from zap events; rather, the total amount of punishment events actually stays the same or even increases with **CNM**. Remember zapping can also be used instrumentally, e.g., to compete over berries or apples. Fig. 5 shows the average number of zaps in an episode summed over the agents for *AH* and *CSP*. Note that there is no observable amount of difference in the net amount of zapping for *AH* and zapping increases for *CSP*. Thus, improvements in collective return must be coming from changes in how zapping is used.

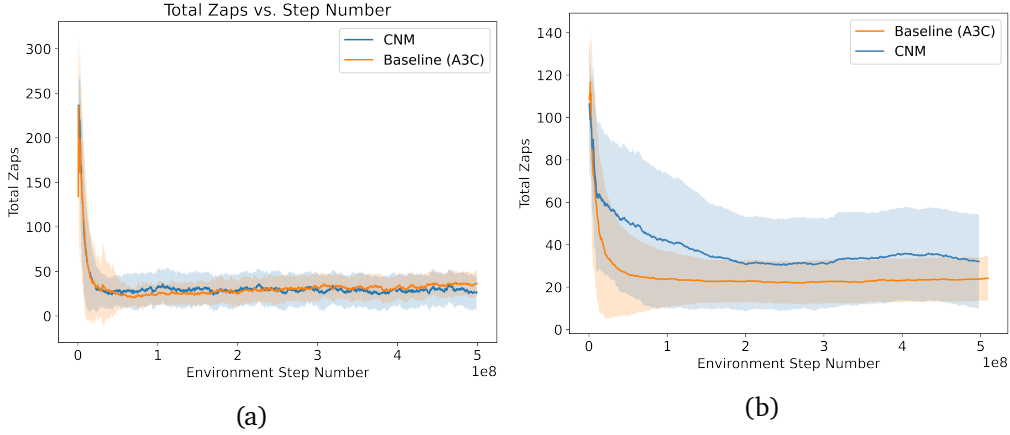


Figure 5 | Effect of CNM on total number of zaps averaged across seeds in (a) *AH* (b) *CSP*.

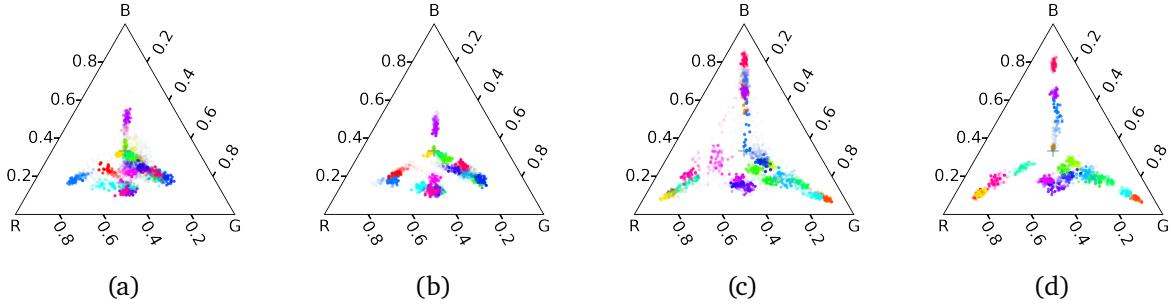


Figure 6 | Evidence of stable planting behavior after $2e8$ steps of training. Individual dots are samples over a run where darker dots represent later points. (a) First $2e8$ steps with **CNM** off. (b) Latter $2.5e8$ steps with **CNM** off. (c) First $2e8$ steps with **CNM** on. (d) Latter $2.5e8$ steps with **CNM** on.

5.2. How does CNM establish social norms?

Here we show that **CNM** increases incentives to obey social norms i.e. agents are disapproved of more for deviating from working toward the established equilibrium relative to how much they are disapproved of for free riding or working toward other equilibria. In *AH*, the equilibria are likely given by the corners of the berry fraction simplex (Fig. 6). Stabilization comes from disapproval of re-planting behaviors that would otherwise push the system away from equilibrium. We can approximately observe stability in the planting behavior by examining the evolution of the fraction of each berry color on the simplex. Fig. 6 demonstrates the changes in the evolution of berry fraction during early and late phases of training. Here the center of the diagram indicates that either all agents are free-riding or that they are all cancelling out one another’s planting behavior (e.g. I change a red berry to blue and you change a blue berry to red so there is no net effect on the berry fractions). We observe that groups of **CNM** agents push further away from the center and towards the corners of the simplex. Furthermore, there is little change in later steps of training for the seeds that reach the simplex corners, suggesting an equilibrium. There is some small amount of drift in high blue monoculture fraction runs which may be attributable to the fact that the blue berries are not preferred by any agent.

The second criterion to check concerning the establishment of a social norm is that deviations from the equilibrium should be disapproved (sanctioned). We can calculate for each color $p(\text{zapped} \mid \text{color})$ by Bayes’ rule (details in Appendix). We then use it to investigate the sanctioning

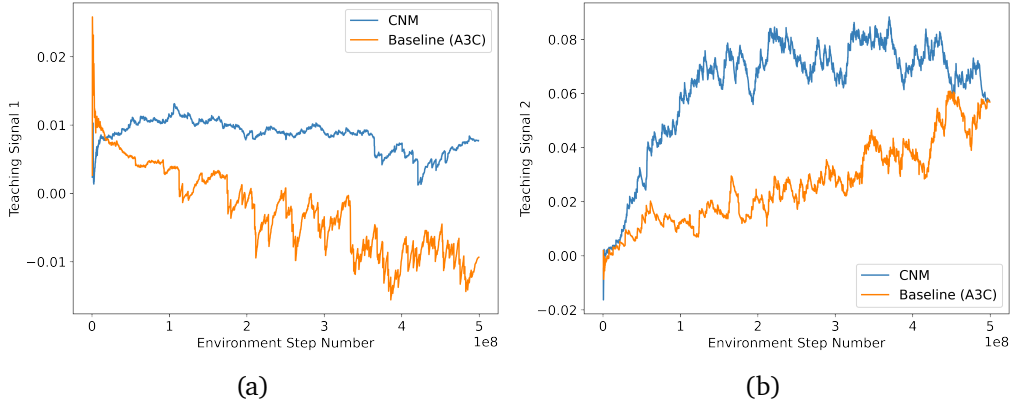


Figure 7 | Measurements of the strength of disapproving sanctions applied to deviating agents in allelopathic harvest: (a) difference between zap likelihood for being the free-rider color vs. being the dominant color (b) difference of zap likelihood for being the second most dominant color to being the dominant color.

forces supporting a particular equilibrium by looking at the difference in log likelihood of being punished while working toward establishing or maintaining the equilibrium. Agents can readily perceive which equilibrium other agents in their field of view are supporting because their color shows which color berry they last planted (see Section 4). If the likelihood difference for a particular color is high it should be easy for the learning algorithm to identify that switching to that color (i.e. switching to support its corresponding equilibrium) is likely to lead to disapproval. Thus, these differences serve as a teaching signal pushing the agent towards planting one color and away from planting another.

Fig. 7 demonstrates this effect for two different potential switches. Fig. 7a measures the difference of punishment likelihood between free-riding and planting the dominant color which we call *teaching signal 1*. If the magnitude of this signal is large and positive, it is easy for the learning algorithm to identify that switching from free-riding to planting in that color will decrease the amount that it gets punished.

Fig. 7b measures the relative likelihood of getting punished when we plant the color corresponding to high monoculture versus if we were to switch to plant the second most abundant berry color which we refer to as *teaching signal 2*. If this signal is large, it is easier for the learning algorithm to identify that sticking to the dominant color will allow it to decrease how often it gets disapproved of which in turn will help stabilize the choice of equilibrium.

5.3. Ablations on architecture components

To understand CNM better we gradually remove and alter components of the architecture to answer the following questions: (1) Is freezing the classifier necessary? (2) Is it essential to learn social norms from global sanctions or will local sanctions observed by each individual themselves suffice? (3) Is our result sensitive to the relative scale between approval and disapproval pseudorewards?

Here we study CSP as the smaller number of agents in this environment decreases environment step time and allows us to perform more rapid experimentation. We run each ablation over ten seeds. For point (1), we allow the classifier to continue learning throughout training. For (2) we train the classifier using only the sanctioning events directly observed by each agent. Finally, for (3), we note that in all prior experiments we have scaled the pseudorewards so that the penalty for punishing discordantly with the classifier (β) is twice the reward for punishing in accord with it (α). We aim to

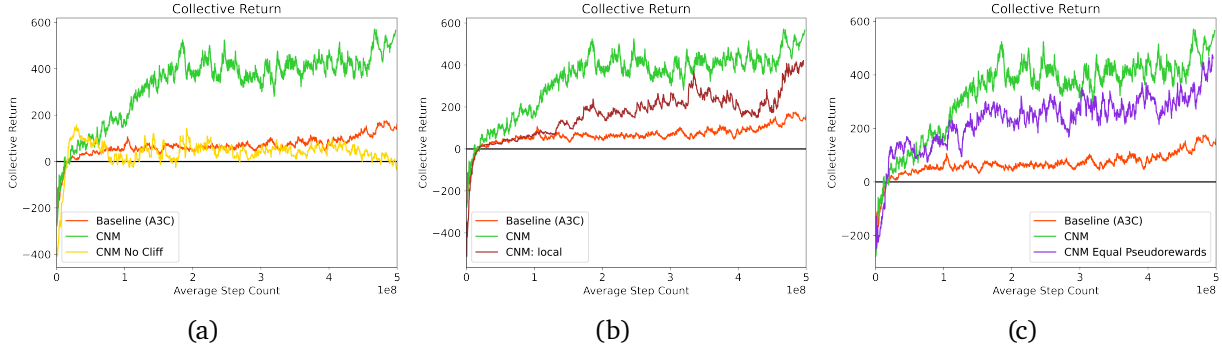


Figure 8 | Ablations of key components of the agent architecture. (a) The classifier is not frozen during training. (b) The classifier is learned solely from sanctions experienced by the agent i.e sanctions are private. (c) Effect of pseudoreward scale; both α and β are set to 0.9.

establish whether our results are sensitive to this particular ratio.

Fig. 8 demonstrates the outcome of all of these ablations; each curve is the average across ten seeds with std. deviations removed for visual clarity. In Fig. 8a we can see that in the absence of a frozen classifier the collective return experiences a large early spike but then decays quickly down. While we are unable to definitively establish the mechanism that forces us to freeze the classifier, there are a few plausible ones. The move away from free-riding occurs rapidly in the first $1e8$ steps of training (see Appendix Sec. C). If the punishment behavior is not correspondingly suppressed quickly enough, agents performing cooperative behavior will still get punished due to exploratory noise and the classifier will consequently learn to recommend punishment of cooperative agents. Alternately, the classifier could simply experience *catastrophic forgetting* once a particular color is effectively suppressed: it’s difficult to remember how to sanction a behavior that no longer occurs. Consequently, the suppressed behavior is able to re-emerge.

In Fig. 8b we observe that learning solely from local sanctions does improve over the baseline but does not completely match the performance of fully public sanctions. Since the agents have to infer the norm solely through agents they happen to interact with, the number of samples available for each classifier update decreases sharply which may make the subsequent learned norm noisier and harder to learn. Finally, in Fig. 8c we set the pseudorewards to a magnitude of 0.9 for both approval and disapproval. We note that this is less than the potential reward of consuming an apple, making it feasible for an agent to zap discordantly to the recommendation of the classifier if doing so nets them an additional apple. We see that there is a slight reduction in the collective return but there remains an improvement over the A3C baseline.

6. Discussion and Future Work

Motivated by emerging challenges in deploying autonomous systems, we introduce and formalize a new training regime for decentralized multi-agent learning in which all sanctions are publicly observable. We observe that in this setting baseline decentralized agents struggle to achieve cooperative behavior in the collective action problems posed by two environments that broadly model challenges of free-riding and equilibrium selection. Inspired by social norms, which humans often use to overcome such dilemmas, we introduce an agent architecture: **CNM**, that operates in this setting. It learns to classify and enforce social norms from experience. We show that groups of **CNM** agents converge on beneficial equilibria and are better at resolving free-rider problems than agents implementing a baseline algorithm.

In contrast to centralized training methods, **CNM** can be trained fully online without needing access to a simulator. Thus **CNM** may make it easier to satisfy privacy constraints since potentially sensitive data like rewards and policies do not need to be shared to achieve cooperation and coordination.⁶

Many potentially fruitful avenues for further research using **CNM** remain open. For instance, the architecture used for the classifier, a convolutional network, relies on there being an identifiable visual cue that correlates with the behavior to be made normative. Thus it is restricted in the types of norms it can identify. An extended **CNM** architecture operating on snippets of video preceding each sanctioning event may allow for different social norms to emerge.

Furthermore, while we observe the appearance of seemingly stable, beneficial norms, we do not provide a complete mechanistic explanation of how this architecture selects and stabilizes equilibria. It is possible that there exist games where this architecture would exclusively select harmful norms or deeply unfair norms. From the standpoint of using **CNM** for social science modeling, this is a feature not a bug. In the real world, for every beneficial norm enabling collective action, there are hosts of unsavory norms (but see also [Hadfield-Menell et al. \(2019\)](#); [Köster et al. \(2020a\)](#)). Moreover, we must not take for granted that social norms are always a desirable outcome for a multi-agent system. For instance, social norms impose a deadweight loss due to the effort needed to maintain them. Paying this cost may not always be worthwhile in all applications. Nevertheless, we believe that **CNM**, or a successor system, could eventually be employed fruitfully in a wide range of applications from social science modeling to real-world multi-agent systems where interfacing with human social norms is especially critical.

⁶Note though that **CNM** is not a privacy panacea. It eschews sharing simulators, rewards, and policies, but encourages instead the public sharing of sanctioning contexts. These may also contain sensitive information. However, as long as user unwillingness to share data due to privacy concerns and user sanctioning behavior are uncorrelated, the resulting set of sanctioning examples will still be descriptive of user behavior. Furthermore, sanctioning contexts could be anonymized using techniques such as DeepObfuscator ([Li et al., 2019](#)).

References

- G. Akerlof. The economics of caste and of the rat race and other woeful tales. *The Quarterly Journal of Economics*, pages 599–617, 1976.
- B. Baker. Emergent reciprocity and team formation from randomized uncertain social preferences. In *Advances in Neural Information Processing Systems 33: Annual Conference on Neural Information Processing Systems 2020, NeurIPS 2020, December 6-12, 2020, virtual*, 2020. URL <https://proceedings.neurips.cc/paper/2020/hash/b63c87b0a41016ad29313f0d7393cee8-Abstract.html>.
- L. Balafoutas, N. Nikiforakis, and B. Rockenbach. Direct and indirect punishment among strangers in the field. *Proceedings of the National Academy of Sciences*, 111(45):15924–15927, 2014.
- D. A. Baldwin. The power of positive sanctions. *World Politics*, 24(1):19–38, 1971.
- C. Bicchieri. *The grammar of society: The nature and dynamics of social norms*. Cambridge University Press, 2006.
- C. Bicchieri. *Norms in the wild: How to diagnose, measure, and change social norms*. Oxford University Press, 2016.
- C. Bicchieri, R. Muldoon, and A. Sontuoso. Social Norms. In *The Stanford Encyclopedia of Philosophy*. Metaphysics Research Lab, Stanford University, Winter 2018 edition, 2018.
- C. Boehm. *Moral origins: The evolution of virtue, altruism, and shame*. Soft Skull Press, 2012.
- R. Boyd and S. Mathew. Arbitration supports reciprocity when there are frequent perception errors. *Nature Human Behaviour*, pages 1–8, 2021.
- M. Carroll, R. Shah, M. K. Ho, T. Griffiths, S. A. Seshia, P. Abbeel, and A. D. Dragan. On the utility of learning about humans for human-ai coordination. In H. M. Wallach, H. Larochelle, A. Beygelzimer, F. d’Alché-Buc, E. B. Fox, and R. Garnett, editors, *Advances in Neural Information Processing Systems 32: Annual Conference on Neural Information Processing Systems 2019, NeurIPS 2019, December 8-14, 2019, Vancouver, BC, Canada*, pages 5175–5186, 2019.
- S. Çolak, A. Lima, and M. C. González. Understanding congested travel in urban areas. *Nature communications*, 7(1):1–8, 2016.
- J. W. Crandall, M. Oudah, F. Ishowo-Oloko, S. Abdallah, J.-F. Bonnefon, M. Cebrian, A. Shariff, M. A. Goodrich, I. Rahwan, et al. Cooperating with machines. *Nature communications*, 9(1):1–12, 2018.
- T. Eccles, E. Hughes, J. Kramár, S. Wheelwright, and J. Z. Leibo. Learning reciprocity in complex sequential social dilemmas. *arXiv preprint arXiv:1903.08082*, 2019.
- L. Espeholt, H. Soyer, R. Munos, K. Simonyan, V. Mnih, T. Ward, Y. Doron, V. Firoiu, T. Harley, I. Dunning, et al. Impala: Scalable distributed deep-rl with importance weighted actor-learner architectures. In *International Conference on Machine Learning*, pages 1407–1416. PMLR, 2018.
- E. Fehr and U. Fischbacher. Social norms and human cooperation. *Trends in cognitive sciences*, 8(4): 185–190, 2004.
- J. Foerster, R. Y. Chen, M. Al-Shedivat, S. Whiteson, P. Abbeel, and I. Mordatch. Learning with opponent-learning awareness. In *Proceedings of the 17th International Conference on Autonomous Agents and MultiAgent Systems*, pages 122–130, 2018a.

- J. Foerster, G. Farquhar, T. Afouras, N. Nardelli, and S. Whiteson. Counterfactual multi-agent policy gradients. In *Proceedings of the AAAI Conference on Artificial Intelligence*, volume 32, 2018b.
- I. Gemp, K. R. McKee, R. Everett, E. A. Duéñez-Guzmán, Y. Bachrach, D. Balduzzi, and A. Tacchetti. D3c: Reducing the price of anarchy in multi-agent learning. *arXiv preprint arXiv:2010.00575*, 2020.
- H. Gintis. Social norms as choreography. *politics, philosophy & economics*, 9(3):251–264, 2010.
- M. Granovetter. Threshold models of collective behavior. *American journal of sociology*, 83(6): 1420–1443, 1978.
- G. K. Hadfield and B. R. Weingast. What is law? a coordination model of the characteristics of legal order. *Journal of Legal Analysis*, 4(2):471–514, 2012.
- G. K. Hadfield and B. R. Weingast. Law without the state: legal attributes and the coordination of decentralized collective punishment. *Journal of Law and Courts*, 1(1):3–34, 2013.
- G. K. Hadfield and B. R. Weingast. Microfoundations of the rule of law. *Annual Review of Political Science*, 17:21–42, 2014.
- D. Hadfield-Menell, M. Andrus, and G. Hadfield. Legible normativity for ai alignment: The value of silly rules. In *Proceedings of the 2019 AAAI/ACM Conference on AI, Ethics, and Society*, pages 115–121, 2019.
- D. D. Heckathorn. The dynamics and dilemmas of collective action. *American sociological review*, pages 250–277, 1996.
- J. Henrich and M. Muthukrishna. The origins and psychology of human cooperation. *Annual Review of Psychology*, 72:207–240, 2021.
- E. Hughes, J. Z. Leibo, M. Phillips, K. Tuyls, E. A. Duéñez-Guzmán, A. G. Castañeda, I. Dunning, T. Zhu, K. R. McKee, R. Koster, H. Roff, and T. Graepel. Inequity aversion improves cooperation in intertemporal social dilemmas. In *Advances in Neural Information Processing Systems 31: Annual Conference on Neural Information Processing Systems 2018, NeurIPS 2018, December 3-8, 2018, Montréal, Canada*, pages 3330–3340, 2018. URL <https://proceedings.neurips.cc/paper/2018/hash/7fea637fd6d02b8f0adf6f7dc36aed93-Abstract.html>.
- S. Iqbal and F. Sha. Coordinated exploration via intrinsic rewards for multi-agent reinforcement learning. *arXiv preprint arXiv:1905.12127*, 2019.
- M. Jaderberg, V. Mnih, W. M. Czarnecki, T. Schaul, J. Z. Leibo, D. Silver, and K. Kavukcuoglu. Reinforcement learning with unsupervised auxiliary tasks. In *5th International Conference on Learning Representations, ICLR 2017, Toulon, France, April 24-26, 2017, Conference Track Proceedings*. OpenReview.net, 2017a. URL <https://openreview.net/forum?id=SJ6yPD5xg>.
- M. Jaderberg, V. Mnih, W. M. Czarnecki, T. Schaul, J. Z. Leibo, D. Silver, and K. Kavukcuoglu. Reinforcement learning with unsupervised auxiliary tasks. In *5th International Conference on Learning Representations, ICLR 2017, Toulon, France, April 24-26, 2017, Conference Track Proceedings*. OpenReview.net, 2017b. URL <https://openreview.net/forum?id=SJ6yPD5xg>.
- N. Jaques, A. Lazaridou, E. Hughes, C. Gulcehre, P. Ortega, D. Strouse, J. Z. Leibo, and N. De Freitas. Social influence as intrinsic motivation for multi-agent deep reinforcement learning. In *International Conference on Machine Learning*, pages 3040–3049. PMLR, 2019.

- P. Kairouz, H. B. McMahan, B. Avent, A. Bellet, M. Bennis, A. N. Bhagoji, K. Bonawitz, Z. Charles, G. Cormode, R. Cummings, et al. Advances and open problems in federated learning. *arXiv preprint arXiv:1912.04977*, 2019.
- H. H. Kelley, J. G. Holmes, N. L. Kerr, H. T. Reis, C. E. Rusbult, and P. A. Van Lange. *An atlas of interpersonal situations*. Cambridge University Press, 2003.
- R. Köster, D. Hadfield-Menell, G. K. Hadfield, and J. Z. Leibo. Silly rules improve the capacity of agents to learn stable enforcement and compliance behaviors. *arXiv preprint arXiv:2001.09318*, 2020a.
- R. Köster, K. R. McKee, R. Everett, L. Weidinger, W. S. Isaac, E. Hughes, E. A. Duéñez-Guzmán, T. Graepel, M. Botvinick, and J. Z. Leibo. Model-free conventions in multi-agent reinforcement learning with heterogeneous preferences. *arXiv preprint arXiv:2010.09054*, 2020b.
- A. Lacoste, A. Luccioni, V. Schmidt, and T. Dandres. Quantifying the carbon emissions of machine learning. *arXiv preprint arXiv:1910.09700*, 2019.
- M. Lanctot, V. Zambaldi, A. Gruslys, A. Lazaridou, K. Tuyls, J. Pérolat, D. Silver, and T. Graepel. A unified game-theoretic approach to multiagent reinforcement learning. *arXiv preprint arXiv:1711.00832*, 2017.
- J. Z. Leibo, V. Zambaldi, M. Lanctot, J. Marecki, and T. Graepel. Multi-agent Reinforcement Learning in Sequential Social Dilemmas. In *Proceedings of the 16th International Conference on Autonomous Agents and Multiagent Systems (AA-MAS 2017)*, Sao Paulo, Brazil, 2017.
- J. Z. Leibo, E. Hughes, M. Lanctot, and T. Graepel. Autocurricula and the emergence of innovation from social interaction: A manifesto for multi-agent intelligence research. *arXiv preprint arXiv:1903.00742*, 2019.
- J. Z. Leibo, E. A. Dueñez-Guzman, A. Vezhnevets, J. P. Agapiou, P. Sunehag, R. Koster, J. Matyas, C. Beattie, I. Mordatch, and T. Graepel. Scalable evaluation of multi-agent reinforcement learning with melting pot. In *International Conference on Machine Learning*, pages 6187–6199. PMLR, 2021.
- D. Lewis. *Convention*. Harvard University Press, 1969.
- A. Li, J. Guo, H. Yang, F. D. Salim, and Y. Chen. Deepobfuscator: Obfuscating intermediate representations with privacy-preserving adversarial learning on smartphones. *arXiv preprint arXiv:1909.04126*, 2019.
- X. Liang, Y. Liu, T. Chen, M. Liu, and Q. Yang. Federated transfer reinforcement learning for autonomous driving. *arXiv preprint arXiv:1910.06001*, 2019.
- M. L. Littman. Markov games as a framework for multi-agent reinforcement learning. In *Proceedings of the 11th International Conference on Machine Learning (ICML)*, pages 157–163, 1994.
- R. Lowe, Y. Wu, A. Tamar, J. Harb, P. Abbeel, and I. Mordatch. Multi-agent actor-critic for mixed cooperative-competitive environments. In *Proceedings of the 31st International Conference on Neural Information Processing Systems*, pages 6382–6393, 2017.
- A. Lupu and D. Precup. Gifting in multi-agent reinforcement learning. In *Proceedings of the 19th International Conference on Autonomous Agents and MultiAgent Systems*, pages 789–797, 2020.
- G. Mackie. Ending footbinding and infibulation: A convention account. *American sociological review*, pages 999–1017, 1996.

- G. Marwell and P. Oliver. *The Critical Mass in Collective Action*. Cambridge University Press, 1993.
- S. McAleer, J. Lanier, P. Baldi, and R. Fox. Xdo: A double oracle algorithm for extensive-form games. *arXiv preprint arXiv:2103.06426*, 2021.
- J. L. McClelland, B. L. McNaughton, and R. C. O’Reilly. Why there are complementary learning systems in the hippocampus and neocortex: insights from the successes and failures of connectionist models of learning and memory. *Psychological review*, 102(3):419, 1995.
- K. R. McKee, I. Gemp, B. McWilliams, E. A. Duñez-Guzmán, E. Hughes, and J. Z. Leibo. Social diversity and social preferences in mixed-motive reinforcement learning. In *Proceedings of the 19th International Conference on Autonomous Agents and MultiAgent Systems*, pages 869–877, 2020.
- V. Mnih, A. P. Badia, M. Mirza, A. Graves, T. Lillicrap, T. Harley, D. Silver, and K. Kavukcuoglu. Asynchronous methods for deep reinforcement learning. In *International conference on machine learning*, pages 1928–1937. PMLR, 2016.
- K. Nyborg, J. M. Anderies, A. Dannenberg, T. Lindahl, C. Schill, M. Schlüter, W. N. Adger, K. J. Arrow, S. Barrett, S. Carpenter, et al. Social norms as solutions. *Science*, 354(6308):42–43, 2016.
- M. Olson. *The Logic of Collective Action: Public Goods and the Theory of Groups, Second Printing with a New Preface and Appendix*, volume 124. Harvard University Press, 1965.
- A. v. d. Oord, Y. Li, and O. Vinyals. Representation learning with contrastive predictive coding. *arXiv preprint arXiv:1807.03748*, 2018.
- E. Ostrom. A behavioral approach to the rational choice theory of collective action: Presidential address, american political science association, 1997. *American political science review*, 92(1):1–22, 1998.
- E. Ostrom. *Understanding institutional diversity*. Princeton university press, 2009.
- J. Pérolat, J. Z. Leibo, V. F. Zambaldi, C. Beattie, K. Tuyls, and T. Graepel. A multi-agent reinforcement learning model of common-pool resource appropriation. In *Advances in Neural Information Processing Systems 30: Annual Conference on Neural Information Processing Systems 2017, December 4-9, 2017, Long Beach, CA, USA*, pages 3643–3652, 2017. URL <https://proceedings.neurips.cc/paper/2017/hash/2b0f658cbffd284984fb11d90254081f-Abstract.html>.
- A. Peysakhovich and A. Lerer. Prosocial learning agents solve generalized stag hunts better than selfish ones. In *Proceedings of the 17th International Conference on Autonomous Agents and MultiAgent Systems*, pages 2043–2044, 2018.
- E. A. Platanios, A. Saparov, and T. Mitchell. Jelly bean world: A testbed for never-ending learning. In *International Conference on Learning Representations*, 2019.
- T. Rashid, M. Samvelyan, C. Schroeder, G. Farquhar, J. Foerster, and S. Whiteson. Qmix: Monotonic value function factorisation for deep multi-agent reinforcement learning. In *International Conference on Machine Learning*, pages 4295–4304. PMLR, 2018.
- S. Sen and S. Airiau. Emergence of norms through social learning. In *IJCAI*, volume 1507, page 1512, 2007.
- L. S. Shapley. Stochastic Games. In *Proc. of the National Academy of Sciences of the United States of America*, 1953.

- Y. Shoham and M. Tennenholtz. On the emergence of social conventions: modeling, analysis, and simulations. *Artificial Intelligence*, 94(1-2):139–166, 1997.
- S. Singh, A. G. Barto, and N. Chentanez. Intrinsically motivated reinforcement learning. In *Proceedings of the 17th International Conference on Neural Information Processing Systems*, pages 1281–1288, 2004.
- K. O. Stanley. Why open-endedness matters. *Artificial life*, 25(3):232–235, 2019.
- P. Sunehag, G. Lever, A. Gruslys, W. M. Czarnecki, V. Zambaldi, M. Jaderberg, M. Lanctot, N. Sonnerat, J. Z. Leibo, K. Tuyls, et al. Value-decomposition networks for cooperative multi-agent learning based on team reward. In *Proceedings of the 17th International Conference on Autonomous Agents and MultiAgent Systems*, pages 2085–2087, 2018.
- M. Tomasello and A. Vaish. Origins of human cooperation and morality. *Annual review of psychology*, 64:231–255, 2013.
- E. Ullmann-Margalit. *The emergence of norms*. Oxford University Press, 1977/2015.
- P. Vanderschraaf. Convention as correlated equilibrium. *Erkenntnis*, 42(1):65–87, 1995.
- A. Vezhnevets, Y. Wu, M. Eckstein, R. Leblond, and J. Z. Leibo. Options as responses: Grounding behavioural hierarchies in multi-agent reinforcement learning. In *International Conference on Machine Learning*, pages 9733–9742. PMLR, 2020.
- W. G. Walter. A machine that learns. *Scientific American*, 185(2):60–64, 1951.
- J. X. Wang, E. Hughes, C. Fernando, W. M. Czarnecki, E. A. Duéñez-Guzmán, and J. Z. Leibo. Evolving intrinsic motivations for altruistic behavior. In *Proceedings of the 18th International Conference on Autonomous Agents and MultiAgent Systems*, pages 683–692, 2019.
- W. Z. Wang, M. Beliaev, E. Biyik, D. A. Lazar, R. Pedarsani, and D. Sadigh. Emergent prosociality in multi-agent games through gifting. In *30th International Joint Conference on Artificial Intelligence (IJCAI)*, 8 2021.
- P. Wiessner. Norm enforcement among the ju/'hoansi bushmen. *Human Nature*, 16(2):115–145, 2005.
- E. Xiao and D. Houser. Emotion expression in human punishment behavior. *Proceedings of the National Academy of Sciences*, 102(20):7398–7401, 2005.
- H. P. Young. The evolution of social norms. *economics*, 7(1):359–387, 2015.

A. Architecture and Algorithmic Details

A.1. Architecture

In the implementation of our agent architecture and algorithm we aimed to stick with configurations proposed in recent work (Köster et al., 2020a). We made sure that they use the same size ConvNets and LSTMs. We didn’t perform any tuning of hyper-parameters and used the ones provided in the original publications studying the environments used here.

The agent’s network consists of a ConvNet with two layers with 16, 32 output channels, kernel shapes 8, 4, and strides 8, 1 respectively. It is followed by an MLP with two layers with 64 neurons each. All activation functions are ReLU and both the ConvNet and the MLP have activations at their final layer. It is followed by an LSTM with 128 units. Policy and baseline (for the critic) are produced by linear layers connected to the output of LSTM.

Our classifier network uses the same architecture as the agent for its ConvNet. However, its MLP is three layers, (64, 64, 2) with the final layer not having an activation applied to its output. A softmax is applied to the output of this MLP to get the predicted probabilities of not-punish and punish respectively where the first index of the output corresponds to the probability of not punishing. As before, all activations in the ConvNet and MLP are ReLUs.

A.2. Classifier Training

For training our classifier, we use batches of data returned by A3C. Each episode is chunked into segments of length 100. For each of these segments, we extract out all the events where

- An agent is able to zap (there is a cooldown period after each zap is used during which time the zap action is unavailable).
- Another agent is within shooting range.

For each of these events, we then look at the action of the agent in the subsequent time-step to acquire a label: 0 for no zap, 1 for zap. Since there are sixteen agents and all sanction events are global, we have up to 1600 possible punishment events in a batch. From these events, we randomly subsample $P = 32$ of the punishment events and $P' = 1024$ of the events where no punishment occurred. If p_i is the classifier output on event i we then form the cross-entropy loss

$$\mathcal{L}_{\text{class}} = \lambda_{\text{class}} \left(\frac{1}{P} \sum_i^P \log(p_i) + \frac{1}{P'} \sum_i^{P'} \log(1 - p_i) \right) \quad (1)$$

where λ_{class} is a scaling factor used to adjust the learning rate of the classifier relative to the learning rate of A3C. The classifier is trained via RMSProp with hyperparameters given in Sec. D.3.

A.3. Motivation to align punishment with group

Given a classifier, we then use its predictions to add a pseudoreward to batches of data returned by A3C. As before, we select all potential sanctioning events. We feed the frame before the sanctioning event to the classifier and generate a prediction. The frame on which the sanctioning event occurs is fed into the policy and the classifier prediction concatenated onto the policy internal state after the MLP and before the LSTM. If the policy outputs a zap action out of its LSTM, we receive a positive reward if the classifier predicted zap as well and a penalty if the classifier predicted not to zap. This process is depicted visually in Fig. 1.

A.4. Algorithm

In addition to the standard A3C loss with the advantages computed using V-Trace (Espeholt et al., 2018), we used an auxiliary loss (Jaderberg et al., 2017b) for shaping the representation using contrastive predictive coding (Oord et al., 2018) (CPC). CPC here discriminates between nearby time points via LSTM state representations (a standard augmentation in recent works with A3C).

Contrastive Predictive Coding Loss:

At a high level, CPC works by taking the input and output of an RNN and trying to predict future RNN outputs from the RNN inputs. It does this over several time-shifts and performs the prediction in a latent space.

Let $q^i \in \mathbb{R}^{L \times B \times N}$ denote the input to the LSTM layer and $q^o \in \mathbb{R}^{L \times B \times N'}$ the output of the RNN where L is the length of the time-slice provided to A3C, B is the batch and N, N' are the dimensions of RNN input and output respectively. For notational convenience, we will write $q_{k:j}$ to denote slices of the matrix q along the time axis i.e. $k : j$ denotes the k 'th to j 'th element along the time axis. We apply a 1-d convolution C with a kernel of size 1 to both input q^i and q^o to project them to a latent dimension of size l , $Cq^i \in \mathbb{R}^{(L*B) \times l}$ where we have folded a matrix reshape into the convolution.

Finally, let \mathcal{L}_{cse} denote the softmax cross-entropy loss and where the loss between a matrix and a matrix will be understood to mean applying the loss element-wise and then computing the mean. The CPC update can then be written as

$$\mathcal{L}_{CPC} = \frac{1}{S} \sum_{i=1}^S \mathcal{L}_{cse} \left(Cq_{s:L}^i (Cq_{0:L-s}^o)^T, \mathbf{I}^{(L-s)*B \times (L-s)*B} \right) \quad (2)$$

Here S represents that we do prediction over all possible time shifts from 1 to S and T is the transpose operation.

B. Environment Details

Here we define the environment dynamics in as much detail as possible. First, a few details that are shared between the two environments. In both environments we will refer to a *grid cell*, which we will define as an (8,8) square of pixels. In both environments the agents have a position and 4 possible rotations that are indexed from 0 to 3 where 0 is North, 1 is East, 2 is South, and 3 is West. Agents can take movement actions where are defined with respect to their current rotation i.e. we have 4 actions Up, Left, Right, Down and when the rotation is 0, Up will move you North whereas when the rotation is 1, Up will move you East.

Both environments contain a zapping beam that can be used to zap agents. Note that the use of this beam is an action that cannot be combined with other actions i.e. if an agent zaps then it cannot also move at that time-step. The zapping beam, as depicted in Fig. 9, extends three grid cells forward from the direction the agent is facing. Additionally, on either side of the agent it also extends three grid cells forward but with the beam emanating from the grid cells directly next to the agent rather than from the grid cell directly in front of the agent. Agents hit by the beam block its forwards progress, as depicted in Fig. 10.

Agents that are zapped by the grid cell acquire a marking, shown in Fig. 10, and are frozen for 25 time-steps. In the frozen state they cannot perform any actions for that duration. If they are zapped again within 50 time-steps, the agent that is zapped receives a reward of -10 (i.e. a penalty) and is removed from the environment for 25 timesteps. During this time, all image based observations will be replaced with an image that is entirely black.



Figure 9 | The zapping beam extended fully.

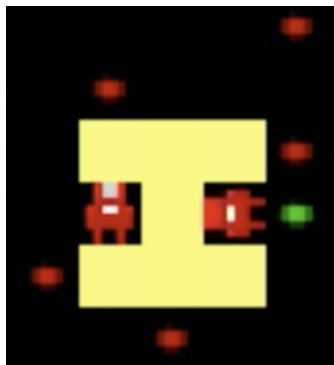


Figure 10 | The zapping beam is blocked due to hitting an agent.

In both environments the observation provided to the policy is an (88, 88, 3) RGB image that is centered on the agent as depicted in Fig. 11 as well as the prediction of the classifier if the classifier is used as discussed in section A.3. The agent sees 9 grid cells in front of it, 1 grid cell behind it, and 5 grid cells to its left and right. Note that "in front, behind, left, right" are all defined with respect to the current rotation of the agent. Cells that fall outside the boundaries of the environment (since the world map is of finite size in Cleanup With Startup Problem) are returned as black.

B.1. Allelopathic Harvest

B.2. Initial Map

At environment reset, the environment is set to the following settings

```

333PPPP12PPP322P32PPP1P13P3P3
1PPPP2PP122PPP3P232121P2PP2P1
P1P3P11PPP13PPP31PPPP23PPPPPP
PPPPP2P2P1P2P3P33P23PP2P2PPPP
P1PPPPPPP2PPP12311PP3321PPPPP
133P2PP2PPP3PPP1PPP2213P112P1
3PPPPPPPPPPPP31PPPPPP1P3112P
PP2P21P21P33PPPPPPPP3PP2PPPP1P
PPPPP1P1P32P3PPP22PP1P2PPPP2P
PPP3PP3122211PPP2113P3PPP1332
PP12132PP1PP1P321PP1PPPPPP1P3
    
```

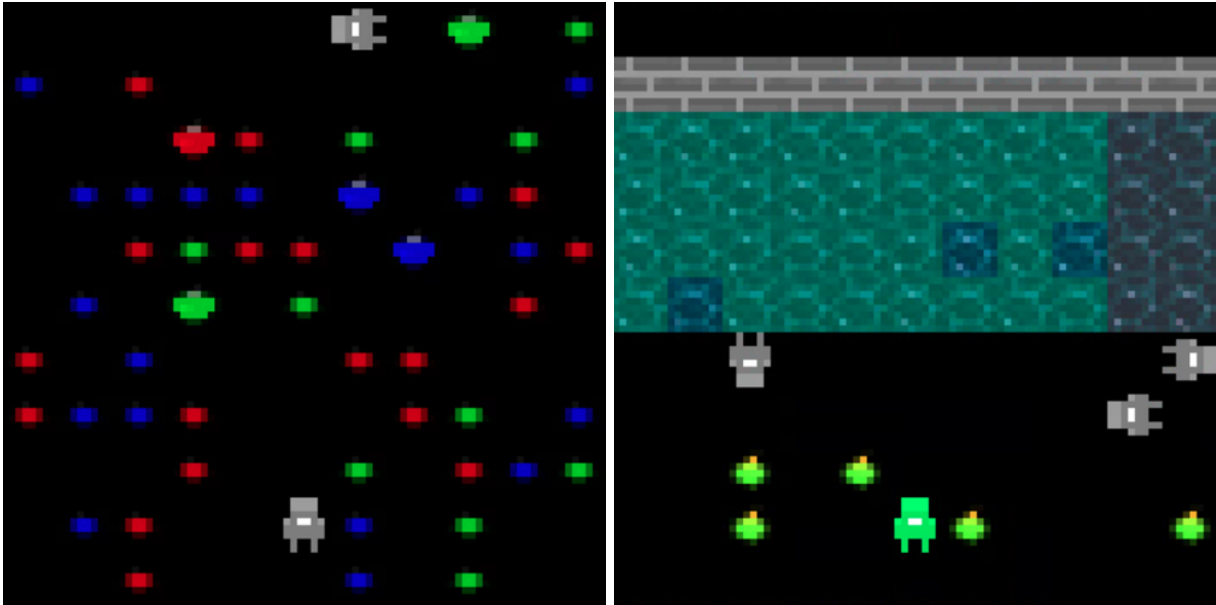


Figure 11 | (Left) Observation of an agent in allelopathic harvest. (Right) Observation of an agent in cleanup.

```

PPP222P12PPPP1PPPP1PPP321P11P
PPP2PPPP3P2P1PPP1P23322PP1P13
23PPP2PPPP2P3PPPP3PP3PPP3PPP2
2PPPP3P3P3PP3PP3P1P3PP11P21P1
21PPP2PP331PP3PPP2PPPPP2PP3PP
P32P2PP2P1PPPPPPP12P2PPP1PPPP
P3PP3P2P21P3PP2PP11PP1323P312
2P1PPPPP1PPP1P2PPP3P32P2P331P
PPPPP1312P3P2PPPP3P32PPPP2P11
P3PPPP221PPP2PPPPPPP1PPP311P
32P3PPPPPPPPPP31PPPP3PPP13PPP
PPP3PPPPP3PPPPPP232P13PPPPP1P
P1PP1PPP2PP3PPPP33321PP2P3PP
P13PPPP1P333PPPP2PP213PP2P3PP
1PPPPP3PP2P1PP21P3PPPP231P2PP
1331P2P12P2PPPP2PPP3P23P21PPP
P3P131P3PPP13P1PPP222PPPP11PP
2P3PPPPPPPP2P323PPP2PPP1PPP2P
21PPPPPPP12P23P1PPPPPP13P3P11
    
```

where P is a position where an agent can be spawned, 1, 2, 3 are berries that are initial set to red, green, and blue respectively. A visual depiction of this map is given in Fig. 12. There are a total of 384 positions where berries can be spawned. There are sixteen agents in the environment at each time (unless one is removed due to a zap), each corresponding to a unique policy.

Action Space

The agent has three additional actions, a re-planting red, green, and blue berry varieties. Technically, these actions are implemented by beams that shoot forward up to three grid cells and are blocked by the first berry they hit, as depicted in Fig. 2. If they hit a differently colored berry, then it gets

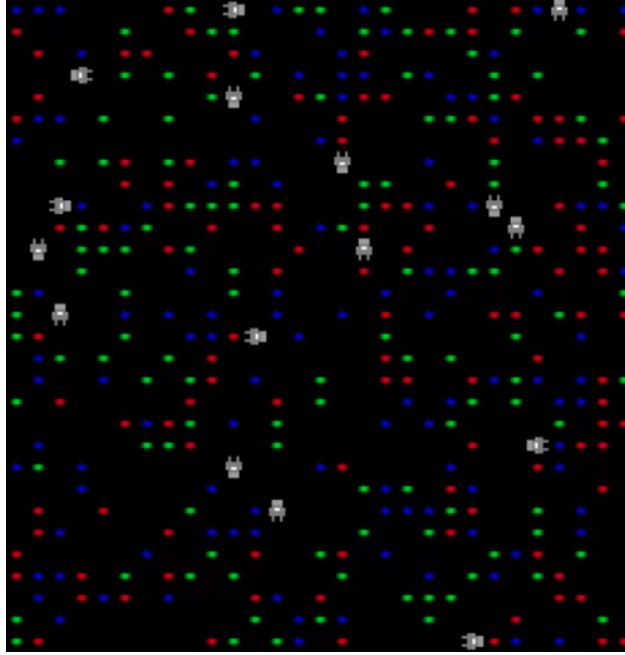


Figure 12 | Allelopathic Harvest map at the first time-step.

replanted with the chosen color berry variety. The replanting actions have a cooldown time and after being used cannot be used again within the next two steps.

Transition Dynamics and Reward Function

Our world map in this environment is a toroid so there is no notion of a boundary of the map and all agent moves (up, left, down, right) and rotations transition the agent to the desired grid cell (unless two agents attempt to enter the same grid cell, in which case the tie is randomly broken). When an agent steps over a berry, that berry is eaten and the agent will receive a reward of 2 if that berry matches its taste preference and a reward of 1 otherwise. Eight of the agents have a taste preference for red and eight have a taste preference for green.

If r , g , b denote the respective numbers of red, green, and blue sites at which berries can spawn, each site of a particular color will spawn a berry at each time-step with probability $0.0000025 * c$ where c is the number of berries of that color. However, a berry cannot be spawned more frequently than every 10 steps and so if a berry has just been eaten, the probability of spawning a berry at that location is 0 until 10 steps have passed. Additionally, berries cannot grow underneath agents, so if an agent remains atop a berry patch no berry will spawn there while the agent stands there.

Agents are initially spawned in colored grey. Agents that successfully change the color of a berry will acquire the new berry color. If those agents then eat a berry, they have some probability of reverting back to grey. If we define the monoculture fraction m as $m = \max\{\frac{r}{r+g+b}, \frac{g}{r+g+b}, \frac{b}{r+g+b}\}$ then the probability of reverting back to grey is $1 - m$. Thus, as the monoculture gets high agents are grey less often. This allows agents to remain colored once they achieve high monoculture fraction, which solves a potential issue wherein monoculture fraction gets high, reducing opportunities to color berries, and agents are then mistakenly identified as free-riders. We observed that without this feature agents would learn to rapidly re-color berries to prevent misidentification as free-riders and added this feature to remove this behavior.

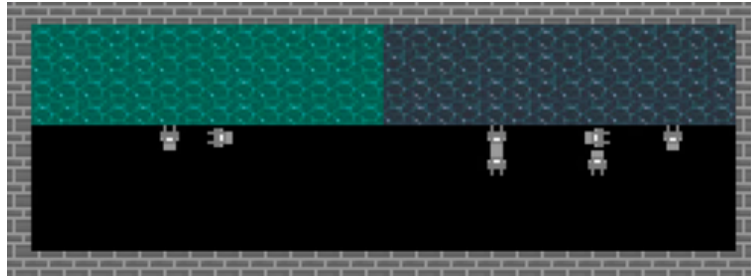


Figure 13 | State of the map at initialization for Clean Up With Start Up Problem

B.3. Cleanup With Startup Problem

Initial Map

An ASCII representation of the initial map is:

```

WWWWWWWWWWWWWWWWWWWWWWWWWWWWWWWWWW
WFFFFFFFFFFFFFFFFDDDDDDDDDDDDDDW
WFFFFFFFFFFFFFFFFDDDDDDDDDDDDDDW
WFFFFFFFFFFFFFFFFDDDDDDDDDDDDDDW
WFFFFFFFFFFFFFFFFDDDDDDDDDDDDDDW
WFFFFFFFFFFFFFFFFDDDDDDDDDDDDDDW
WPPPPPPPPPPPPPPPPPPPPPPPPPPPPPPPW
WPPPPPPPPPPPPPPPPPPPPPPPPPPPPPPPW
WBBBBBBBBBBBBBBBBBBBBBBBBBBBBBBBW
WBBBBBBBBBBBBBBBBBBBBBBBBBBBBBBBW
WBBBBBBBBBBBBBBBBBBBBBBBBBBBBBBBW
WWWWWWWWWWWWWWWWWWWWWWWWWWWWWWWWWW
    
```

where P is a site where agents can initially be spawned on, B is a site where apples can spawn, W is a wall that cannot be passed, F is a cell of pollution type 1 and D is a cell of pollution type 2. An image-based depiction of this is in Fig. 13.

Action Space

The agent has one additional action, a cleaning action. This beam shoots forward up to three grid cells and is blocked by the first bit of pollution it hits. The beam has a cooldown time of 5 seconds. Any cleaned tile has a probability of 0.05 of spawning pollution on it. However, a tile that has been cleaned will not spawn pollution for the first 100 seconds after being cleaned.

Transition Dynamics and Reward Function

As in allelopathic harvest, we wanted to make it possible for agents to eat a few apples without being immediately labelled as a free-rider. Here we add a setting wherein an agent can eat up to 20 berries before being turned gray. If an agent eats 21 berries in a row without cleaning in between, it will turn back to grey.

Now we define the probability function that determines the rates at which apples regrow. If d_1 is the number of uncleaned tiles of color 1 and d_2 is the number of uncleaned tiles of color 2 then the

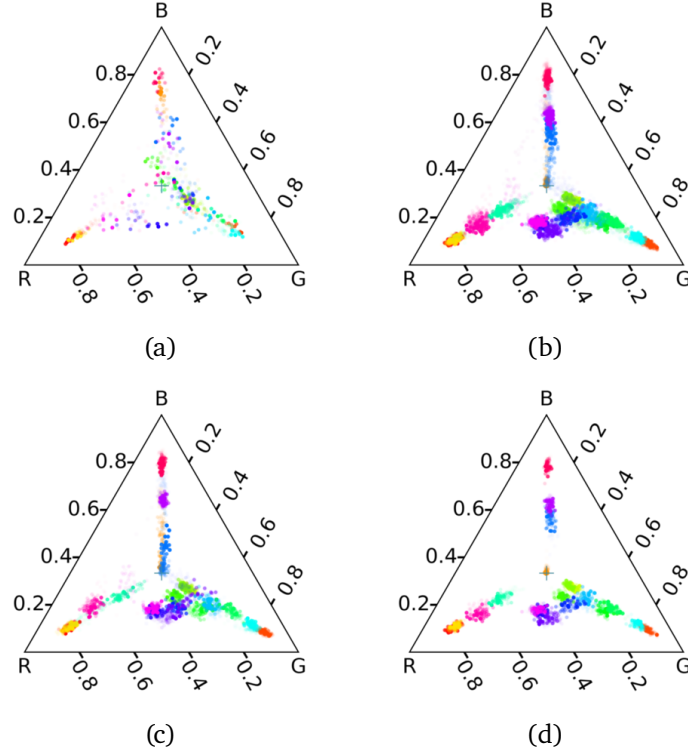


Figure 14 | Evidence of early learning and subsequent semi-stable planting behavior. The cross in the center represents equal berry fractions. Individual dots are samples over a run where darker dots represent later points. (a) First 0 to $5e7$ time-steps. (b) $5e7$ to $1e8$ steps. (c) $1e8$ to $3e8$ steps. (d) $3e8$ to $5e8$ steps.

probability of an apple spawning at any particular site is:

$$0.05 * \left(1 - 0.25 \left(\frac{d_1}{d_1 + d_2} * \frac{d_2}{d_1 + d_2} \right)^{10} \right)$$

This product between the two ratios creates the startup-up problem: if agents equally clear both types of pollution then they are no better off than if they had not cleared any pollution at all. Consuming an apple gives an agent a reward of 1.

C. Learning Dynamics

This section demonstrates that in Allelopathic Harvest, the majority of the learning is confined to the first $1e8$ time-steps with only small changes occurring after that in a few seeds. Fig. 14 demonstrates that the majority of the change in planting behavior occurs early and the later time-steps only change in that 1 seed falls back to full free-riding and a few seeds slightly shift their planting position.

D. Computation Resources and Hyperparameter Tuning

D.1. Tuning Procedure

Here we outline in brief the process by which we arrived at our final set of hyperparameters. The intent of this section is to provide the reader with a sense of the level of tuning that preceded any

common hyperparameters	value
learning rate	$[1e - 4, 1e - 3]$
entropy bonus	$[1e - 3, 1e - 2]$
batch size	16
γ i.e. discount	0.99
number of CPC steps	20
CPC latent space dimension l	64
CPC loss scaling λ_C	10.0
number of CPC steps (S)	20
critic loss scaling λ_{critic}	0.5
RMSProp ϵ	$1e - 5$
RMSProp momentum	0.0
RMSProp decay	0.99
classifier loss scaling λ_{class}	0.01
classifier positive batch size	32
classifier negative batch size	1024

Table 1 | Common hyperparameters used in Allelopathic Harvest and Cleanup With Startup Problem.

final hyperparameter selection. For both A3C and the contrastive predicting coding (CPC) unit we did not perform any tuning of their hyperparameters and only tuned hyperparameters of our classifier and pseudorewards.

Tuning the classifier freeze

The number of actor steps above which training the classifier was frozen was tuned by performing a run without any freezing and observing the point at which the balanced accuracy went above 0.9. For Allelopathic Harvest we only tested a cliff at $1e8$ while for Cleanup With Startup Problem (CSP) we tested cliffs at $0.5e8$ and $1e8$ before settling on $0.5e8$.

D.2. Tuning the size of the pseudorewards

Although for the final experiments we run a fixed size of pseudoreward for each of the environments, there was a heuristic tuning period where we tested a few different hyperparameter magnitudes for each of the environments. Let α refer to the reward for punishing in accord with the classifier and $\beta < 0$ be the penalty for punishing in disaccord with the classifier. Then, for AH we tested early on $(\alpha, \beta) \in \{(0.2, 0.4), (0.4, 0.8), (0.8, 1.6)\}$ and for CSP we tested $(\alpha, \beta) \in \{(1.0, 2.0), (1.2, 2.4)\}$.

D.3. Final Hyperparameters

For both AH and CSP we used the following shared hyper-parameters given in Table. 1 where $[a, b]$ indicates that for a given seed the initial values from the hyperparameter will be drawn from a log-uniform distribution with probability density function $f(x; a, b) = \frac{1}{x[\ln(b) - \ln(a)]}$

The hyperparameters for Allelopathic Harvest are given in Table 2 and for Clean Up With Start Up Problem in Table 3.

Below we outline in more detail what each of the above terms mean.

- Freeze step: After this many environment steps, the classifier learning rate is set to 0.

common hyperparameters	value
α	0.2
β	0.4
Freeze step	1e8

Table 2 | Specific Hyperparameters used in Allelopathic Harvest

common hyperparameters	value
α	1.0
β	2.0
Freeze step	0.5e8

Table 3 | Specific Hyperparameters used in Clean Up With Start Up Problem

- α : the additional reward received when zapping an agent successfully when the classifier predicted a zap.
- β : the penalty received when zapping an agent successfully when the classifier predicted not to zap.

Finally, the loss is formed by combining the sum of the classifier loss, A3C loss, and CPC loss weighted by the loss scalings indicated in Table. 1.

D.4. Computational Resources and Carbon Impact

For each seed of each experiment we use 16 P100 GPUs and 800 CPUs. The Allelopathic Harvest experiments take 2 days to run and the Clean Up experiments take 1 day to run. For Allelopathic Harvest we ran the following experiments:

- 20 seeds for default A3C with no classifier.
- 20 seeds for A3C with the classifier on.

For Clean Up we ran the following experiments:

- 10 seeds for default A3C with no classifier.
- 10 seeds for A3C with the classifier on.
- 10 seeds for each of the 3 ablation experiments.

This gives a total of (20 seeds per experiment) * (2 experiments) * (16 GPUs per experiment) * (2 days per experiment) = 1280 GPU hours for allelopathic harvest and (20 seeds per experiment) * (5 experiments) * (16 GPUs per experiment) * (1 day per experiment) = 1600 GPU hours for cleanup. This gives a total of 2880 GPU hours for the experiments and 144000 CPU hours for the experiments.

Experiments were conducted using an internal GPU cluster, which has a carbon efficiency of 0.27 kgCO₂eq/kWh. Total emissions are estimated to be 403 kgCO₂eq, all of which were directly offset by the GPU cluster provider. Estimations were conducted using the [Machine Learning Impact calculator](#) presented in (Lacoste et al., 2019).